Geochemistry of Clay Dunes and Associated Pan in the Senegal Delta, Mauritania

ABDALLAHI OULD MOHAMEDOU
Faculté des Sciences et Techniques
Nouakchott, Mauritanie

ALAIN AVENTURIER
CIRAD
Unité de Recherches et d'Analyses
Montpellier, France

LAURENT BARBIERO
IRD
Centre de Hann
Dakar, Sénégal

RAOUL CARUBA
IRIM
Université de Nice-Sophia Antipolis
Nice, France

VINCENT VALLES
INRA
Domaine St. Paul, site Agroparc
Avignon, France

Since the construction of the anti-salting Diama dam, a resumption of aeolian defla-tion has been observed in the Senegal delta and particularly in Diawling National Park. It results in the formation of many clay dunes with high salt concentrations. The soft powdery structure observed on the soil surface, affected by aeolian defla-tion is due to rapid salt crystallization. In order to identify the mineralogy of the salt involved in this environment, the chemistry of soil and groundwater was studied along a transect from a pan to the associated clay dune. Equilibria computation and field and scanning electron microscope (SEM) observations indicated that the changes observed in the chemical facies of the solution were due to the following precipitation sequence: calcite > gypsum > halite. A progressive but significant fixing of Na^+ onto the clay particles was observed. The calcite deposition in the soil was limited by exhibition of the potential acidity arising from the former man-grove site soils. It resulted in high equilibrating pCO_2. This study intended to test a new extension to the Debye–Hückel law for concentrated chlorurated sodic waters. The relationship between chloride amounts and the residual alkalinity concept con-firmed that calcite and gypsum formation and the exchanges between Na and Ca are the main phenomena responsible for the changes observed in the soil solution ($r^2 = 0.99$).

Keywords aeolian deflation, lunettes, saline soils, Senegal delta

265

In the Senegal delta the Diama dam was built in 1986 to prevent seawater from flowing upstream in the valley. Since the construction of this reserve dam, clear signs of soil degradation, by increasing salinity, are observed downstream of the dam and particularly in Diawling Park. It results in the disappearance of non-halophile vegetation, and it could induce a drastic decrease in the present seasonal population of birds in the park. From a pedological point of view, a massive resumption of aeolian deflation and clay dune formation is observed. This phenomenon, already noted by many authors in the region, concerns zones that continuously expand from year to year.

Aeolian deflation and clay dune formation have been studied by numerous authors in saline alluvia vallies and particularly in the deltas of West African rivers, such as Senegal and Casamance (Maymard, 1952; Tricart, 1954; Boulaine, 1954; Vieillefon, 1967; Michel, 1973; Mougenot, 1982). The phenomenon of clay dune formation was first explained by Boulaine (1954). Clay dunes develop by seasonal deflation from the pan floor at saline conditions. As the pan dries, salt concentration increases, inducing the mud to flocculate to silt- and sand-size particles, which are then vulnerable to wind transport from the pan floor. According to Hamdi Aissa et al. (1997), this phenomenon is due to the rapid crystallization of salt such as gypsum. The environmental conditions favoring the formation of clay dunes are very specific. They require a prevailing wind during the dry season, temporary saline pan conditions, and a specific clay fraction sediment. Because of these specific conditions, the presence of clay dunes is frequently used for reconstitution of the palaeoenvironment (Hills, 1952; Price, 1963; Bowler, 1973; Lancaster, 1978; Goudie & Thomas, 1984, 1985; Young & Evans, 1986; Thomas, 1988; Thomas et al., 1993; Marker & Holmes, 1995). Bowler (1973) has identified various types of pans according to the mineralogy of salt precipitating during the concentration process. Nevertheless, although the salt has a preponderant role in this type of landscape evolution, little research has been done to determine the processes involved in the development of soil chemical characteristics. This paper is the study of the case of Diawling Park.

Materials and Methods

Site

The study was carried out in Diawling National Park (PND), which covers a narrow triangle between the coast and the Senegal River in southern Mauritania (Figure 1). The park area is 16,000 ha. Two permanent dunes (Birette and Ziré) and mobile dunes along the coast, from Saint Louis in the south to the Chott-boul in the north, constitute the dominant relief in the region. The flooded area of the park consists of the permanently flooded Gambar basin, the Organisation pour la Mise en Valeur du fleuve Sénégal (OMVS) dam reserve, and the periodically flooded Bell basin, whose elevation is higher than that of the Gambar and which includes an estuarian area. Field work was concentrated in Bell basin (16°20'N, 17°25'W), where the process of aeolian deflation is particularly active (Ould Mohamedou, 1998). The climate is characterized by a wet season (average annual precipitation is 170 mm) from July to September, a relatively cold, dry season from October to February (19°C), and a hot, dry season from March to June (37°C). Prevailing winds are from the NNW during the dry season. The studied zone is lightly saline (>7 dS m^{-1}), and much salt efflorescence is observed. The main representative soil is Calcic Gypsic Fluvisol (Food and Agriculture Organization, 1994), but much Thionic Flu-
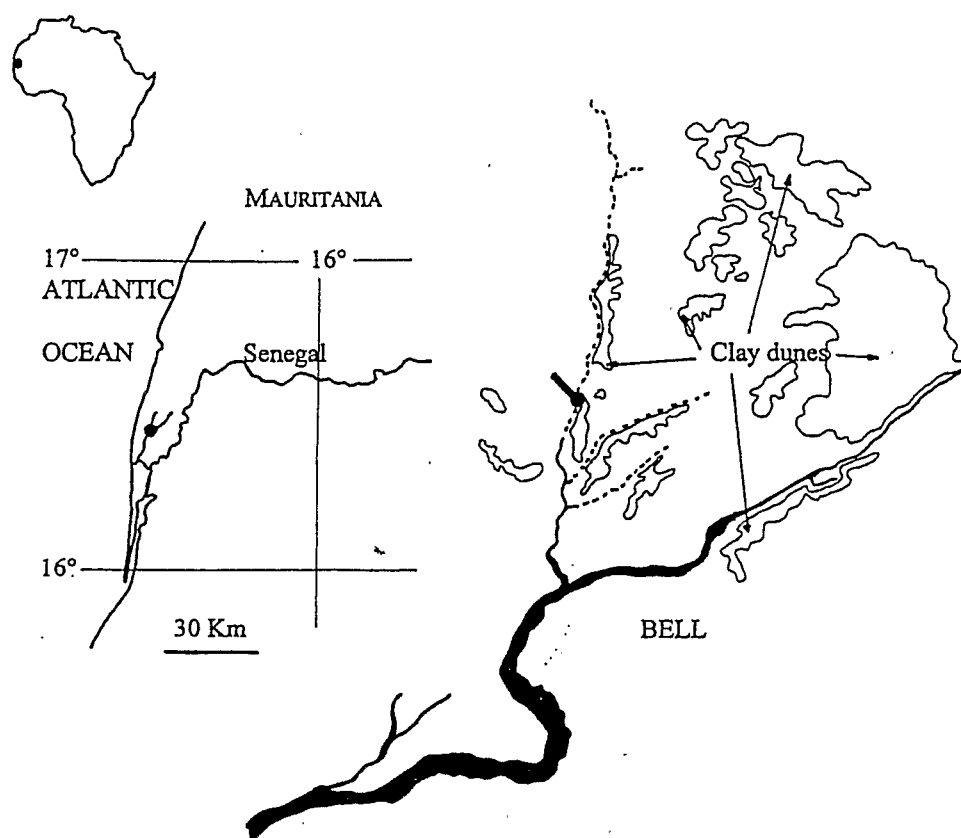
FIGURE 1 Location of the study site in southern Mauritania.

visol containing pyrite (FeS_2) and jarosite [$KFe_3(SO_4)_2(OH)_6$] or natro-jarosite [$NaFe_3(SO_4)_2(OH)_6$] is observed near the remaining mangroves. The high potential acidity of these soils is observed from place to place, as shown by Le Brusq et al. (1987).

The area studied is a plain that is generally flooded from July to September. At the start of flooding, the water is briny because of the salty water ascending from Ncallax Creek and salt deposition. At the end of September, the water becomes diluted with daily variations of the salinity due to the tidal influence. From November to June, salinity of the water and soil increases because of the influence of intense evaporation. Wind deflation occurs on dry soil and results in formation of clay dunes from the accumulation of the particles under the obstacles (mangrove gallery forests, dikes) and around the pans. The phenomenon is important because it gradually confers a singular morphology to the PND landscape.

Sampling

The study was conducted on one of the clay dunes, fringing the Khurumbam Creek, tributary of Bell Creek. Sampling was designed on a transect from the pan to the associated clay dune, 1.5 m high, 30 m wide, and ≈ 2000 m long. The area of the pan is ≈ 18 ha.

The morphology and the soil along the transect (Figure 2) has been reconstituted from 26 borings with a hand auger, and 3 pit descriptions located on lateral soil transition zones. Soil was sampled (94 samples) along this sequence, at depths ranging from 0.1 to 1.3 m. Groundwater was sampled (9 samples) in the water table.

Methods

The pH, electrical conductivity, and temperature of groundwater were measured in the field on nonfiltered samples. The samples were then filtered with a 0.45 μm filter, and total alkalinity was measured in the field by titrating with HCl (Gran, 1952). Solutions were extracted from the saturated pastes of soil samples in the laboratory. The extraction was performed with elevated pressure using filtration modules (cellulose-acetate filters, 0.45 μm). The pH was measured after this filtration.

The major ions Na^+, K^+, Ca^{2+}, Mg^{2+}, and SO_4^{2-} were assessed on both groundwater and soil extracts using emission spectrometry (ICP) (Fassel, 1978). Automatic colorimetry with mercury II thiocyanate at 480 nm was performed for analyzing Cl^- (Charlot, 1961). For saturated paste extracts, the carbonate alkalinity was derived from the chemical balance.

Salt efflorescence was collected for scanning electron microscope (SEM; XL 20 Philips at 15 kV) observations, crystal identification, and analysis using a fitted microprobe (LINK Analytical eXL energy dispersive X-ray system, Philips).

Data Analysis and Activity Coefficient Calculations

Considerations of solution/mineral equilibrium are based on the activity calculation of chemical dissolved ions. This can be measured or estimated from analyses. Many

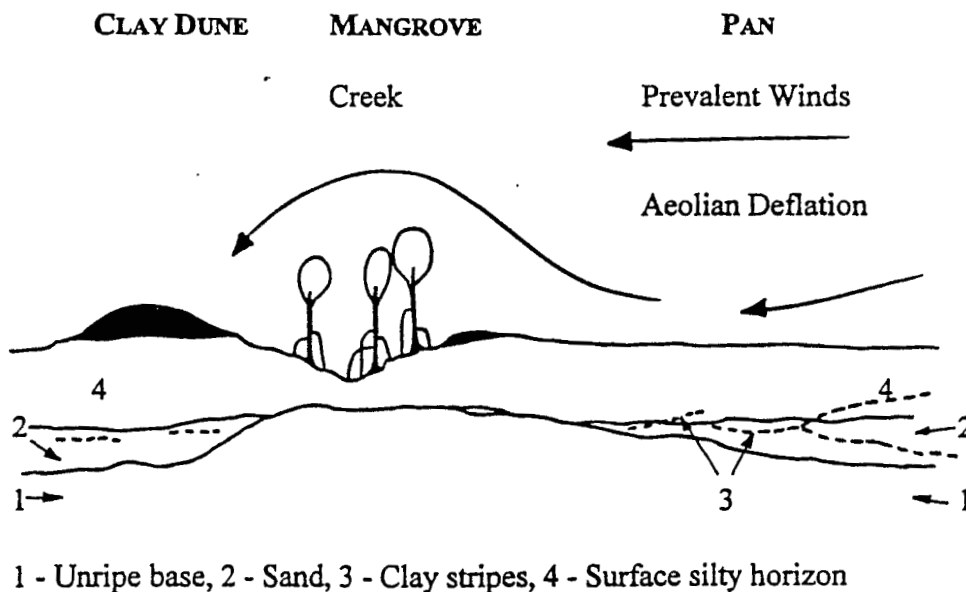1 - Unripe base, 2 - Sand, 3 - Clay stripes, 4 - Surface silty horizon

FIGURE 2 Morphology of the sampled area and distribution of the main horizons.

models exist (Sposito, 1988; Schecher, 1994; Vallès & De Cockerborne, 1992). Similar results are obtained for fresh or moderately concentrated solutions, but the activity calculation can be more or less erroneous in the case of brines. Two types of models are usually used to calculate the activity of ions in a solution.

1. Ion interaction models account for a large number of interactions, from short range or distance to long range, and thus provide accurate estimates of ion activities under strong ionic strengths (≥ 5). These models require many fitting parameters, which are not always available for the type of solution being studied (Pitzer, 1973, 1975; Pitzer & Kim, 1974).

2. Ion pair models have the advantage of requiring no other fitting parameters than the stability constants of the complexes considered. These models are usually built around the Debye–Hückel extension for saline solutions. The Debye–Hückel law itself deals only with electrostatic interactions and gives poor results when applied to brines. Various extensions to it have been suggested. The Scatchard extension (Scatchard, 1936) is among the most commonly used. A more effective extension was recently suggested by Valles et al. (1999). It takes into account the solvent/solute interactions under strong ionic strengths. It was applied successfully to brines in southern Tunisia and Algeria (Valles et al., 1997). This model, called AQUA (Valles & De Cockeborne, 1992), derived from GYPSOL (Valles & Bourgeat, 1988), was used for calculations in the present study.

Definition and Properties of the Generalized Residual Alkalinity

Alkalinity is the sum of the weak base concentrations multiplied by the number of protons each base can neutralize, minus the number of protons in the solution (Stumm & Morgan, 1970; Bourrié, 1976). In most soils the alkalinity is generally due to carbonate species. When evaporation concentrates a solution up to calcite precipitation, two cases may arise. If the calcium equivalent is higher than the carbonate alkalinity, then the calcium molality increases, and alkalinity decreases. If the calcium equivalent is less than the carbonate alkalinity, then molalities change in the opposite direction. After each mineral precipitation, there is a change in the rate of concentration of the elements concerned. By blocking at some natural cases, i.e., when each saturation with respect to a new mineral is reached, the concentration of certain elements can decrease, increase again, or simply fluctuate along the evaporation processes. The concept of residual carbonates originally derived from Eaton (1950) was later redefined in terms of residual alkalinity and generalized to the successive precipitation of several minerals (van Beek & van Breemen, 1973; Al Droubi et al., 1980). More recently, Valles et al. (1991) and Ribolzi et al. (1993, 1996) have shown that the generalized residual alkalinity increases proportionally to the reduction of the solution volume, as a conservative tracer.

Statistical Approach

The data underwent a principal component analysis (PCA) on the following parameters: carbonate alkalinity, K^+, Na^+, Ca^{2+}, Mg^{2+}, Cl^-, and SO_4^{2-}. The PCA was performed considering Cl^- and SO_4^{2-} as supplementary variables because they are closely correlated with Na^+ and Mg^{2+}, respectively.

Results and Discussion

The correlation matrix (Table 1) shows a close relationship between Na^+ and Cl^-. They are the most concentrated elements and indicate the degree of concentration of the solutions. Therefore the main process responsible for chemical variability is the concentration of the dissolved elements. It indicates that all samples belong to the same chemical family. Mg^{2+} is closely correlated to Na^+ and Cl^-, indicating that it is not strongly affected by control processes along the concentration. SO_4^{2-} is less correlated to this group and could have therefore been associated to precipitation/dissolution phenomena. This hypothesis will have to be validated by the study of saturation and concentration diagrams. K^+ and carbonate alkalinity are elements whose concentrations are the most controlled by physicochemical processes.

The singular values examination (Table 2) reveals that the first factorial plan is composed of axes representing 63.3% and 18.4% of the variance of the scattered plot. The first axis opposes elements that are generally feebly controlled: Na^+ and Cl^-, possibly Mg^{2+}, SO_4^{2-} being equally close to this group. It indicates the global concentration of the solutions. The second axis opposes controlled elements, i.e., implied in the chemical process: carbonate alkalinity and calcium. This second factor explains 18.4% of the variance and represents the production/consumption of the alkalinity/acidity in this environment, which is controlled by the sulfide oxidation studied by various authors in the Senegal delta (Le Brusq et al., 1987; Loyer, 1989). The second axis underlines the heterogeneousness of the sulfide oxidation in the sampled zone.

TABLE 1 Correlation matrix of the major ions

	Carbonate alkalinity	K^+	Na^+	Ca^{2+}	Mg^{2+}	Cl^-	SO_4^{2-}
Carbonate alkalinity	1	0.215	0.509	0.251	0.502	0.513	0.337
K^+		1	0.545	0.584	0.606	0.575	0.548
Na^+			1	0.457	0.934	0.993	0.894
Ca^{2+}				1	0.503	0.518	0.331
Mg^{2+}					1	0.958	0.867
Cl^-						1	0.867
SO_4^{2-}							1

TABLE 2 Results of the PCA

Axis	Percentage of the variance v^a	Cumulated percent of the variance
1	63.32	63.32
2	18.37	81.69
3	10.23	91.92
4	6.95	98.87
5	1.13	100

$^a v = (1/n) \sum_{i=1}^{n} (x_i - \bar{x})^2$ and $\bar{x} = (1/n) \sum_{i=1}^{n} x_i$.

Geochemical Processes

The concentration of solutions varied widely. Ionic strength varied from 0.11 to 4.43. Changes in the chemical facies of the solutions were suspected as a function of the concentration factor. Salt-concentrated waters exhibited a chlorurated sodic facies, whereas more salt-diluted waters exhibited a more sulfated calcic and magnesian type. The most diluted solutions had a tendency toward a carbonated calcic facies. However, it appeared that the less concentrated waters could be divided into two groups, one with a chemical facies more sulfated and a little carbonated, the other with a facies less sulfated and more carbonated. This point is discussed below with the study of the equilibrium diagrams.

Concentration Diagrams

Chloride can be used as a conservative tracer to estimate the concentration factor of each solution. This concentration factor is an underestimate if halite (NaCl) precipitates, i.e., eventually for high ionic strength. The concentration diagrams were built under this condition, using Cl^- to estimate the concentration factor.

For the most salt-diluted waters, the calcium amount was higher than the carbonate alkalinity, as illustrated on the stabler diagram (Figure 3). The calcite residual alkalinity was negative. Thus, when solutions concentrate and if calcite precipitates, the calcium molality increases, however less rapidly than chloride ions or sodium molalities because of the calcite precipitation (Figure 4). This evolution was in agreement with the law of the residual alkalinity. However, calcite was scarcely observed in the soil except as shells. More investigation is necessary to estimate the part of the calcite formation in the control of the carbonated alkalinity.

Sulfate amount was controlled coinciding with a control in the calcium curve. It indicated gypsum precipitation. For the moderately salt-concentrated waters when the gypsum precipitated, the sum "sulfate + carbonate alkalinity" was higher than
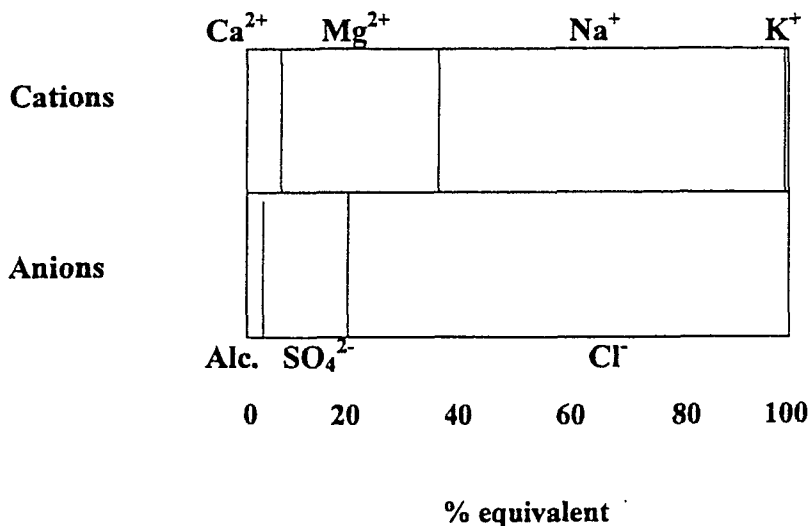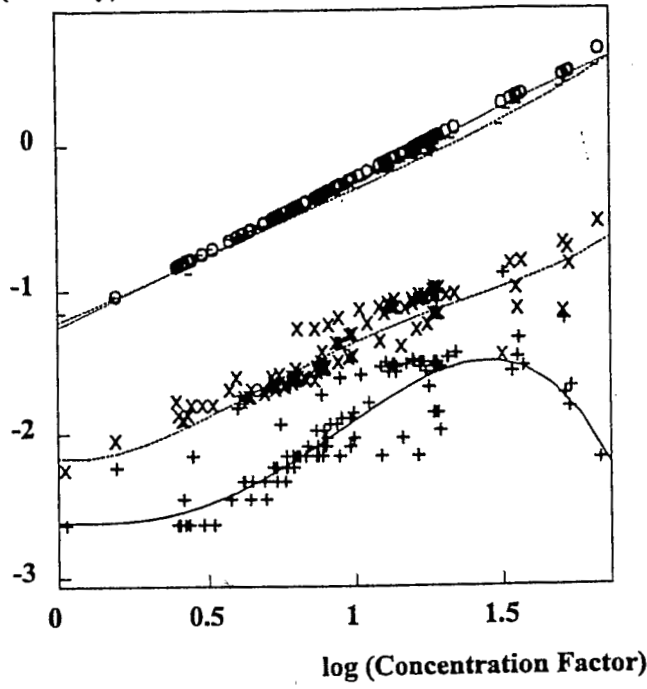

FIGURE 3 Chemical facies of a diluted or moderately concentrated solution.
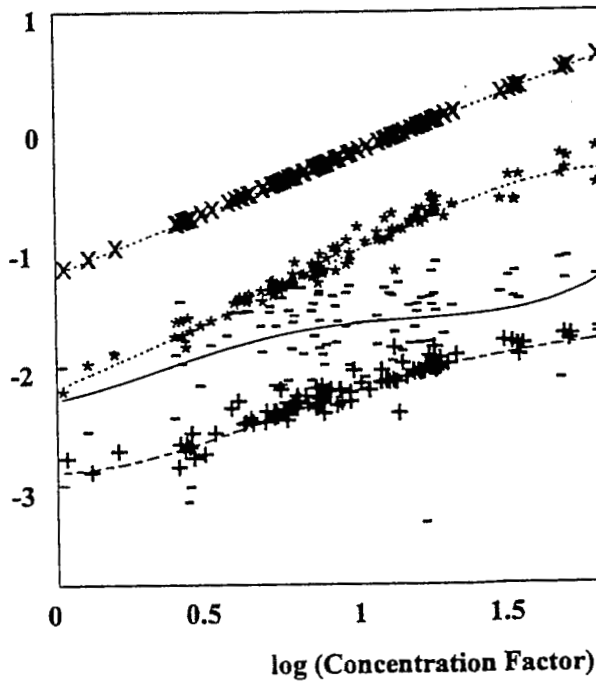
log (molality) **(a)**

x SO4
o Cl
+ Ca
- Na

log (Concentration Factor)

log (molality) **(b)**

.... X Cl
.... * Mg
----- + K
----- - Car. Alk.

log (Concentration Factor)

FIGURE 4 Concentration diagrams according to Cl as the concentration factor.
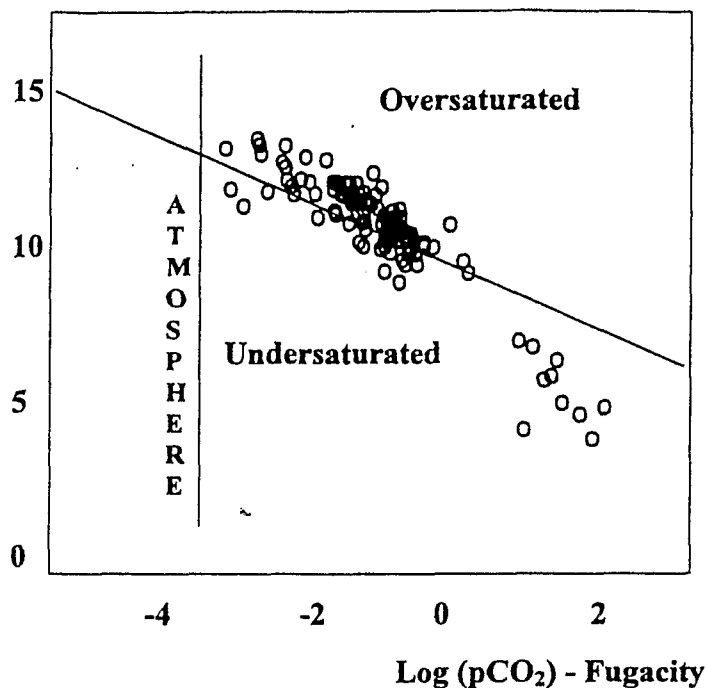
$$\text{Log}(Ca^{2+}) + 2pH + \log(H_2O)$$

FIGURE 5 Saturation diagram with respect to calcite.

the calcium amount. The calcite + gypsum residual alkalinity was positive, as illustrated on Figure 3. Thus the sulfate molality and carbonate alkalinity increased, unlike calcium, in agreement with the residual alkalinity concept.

The following precipitation stage would concern a sodic salt, chlorurated or sulfated. SEM observations on efflorescence from the pan floor or from the clay dune revealed only gypsum and halite, without sodium sulfate salt. Therefore the precipitation sequence calcite > gypsum > halite was probably responsible for the main changes observed in the chemical facies.

The sodium molality appeared moderately controlled, but it increased less rapidly than Cl^-. $Cl^- > Na^+$ for concentrated waters, and $Na^+ > Cl^-$ for moderately concentrated waters. This control of the sodium was progressive. It can be ascribed to progressive fixation of the Na^+ onto clay minerals when soil solutions concentrate and become increasingly sodic. Le Brusq and Loyer (1982) and Mougenot (1982) suspected this phenomenon in the Senegal valley under similar chemical conditions. The evolution of K^+ molalities along the concentration process also has to be interpreted by fixing the exchange complex.

Solution/Mineral Equilibrium Diagrams

The concentration diagrams allow one to interpret the changes in the chemical facies along the concentration process. These interpretations are based on the hypothesis of solution/minerals equilibrium. It is convenient to verify if these equilibria are reached. Solution saturation diagrams are shown for calcite (Figure 5),
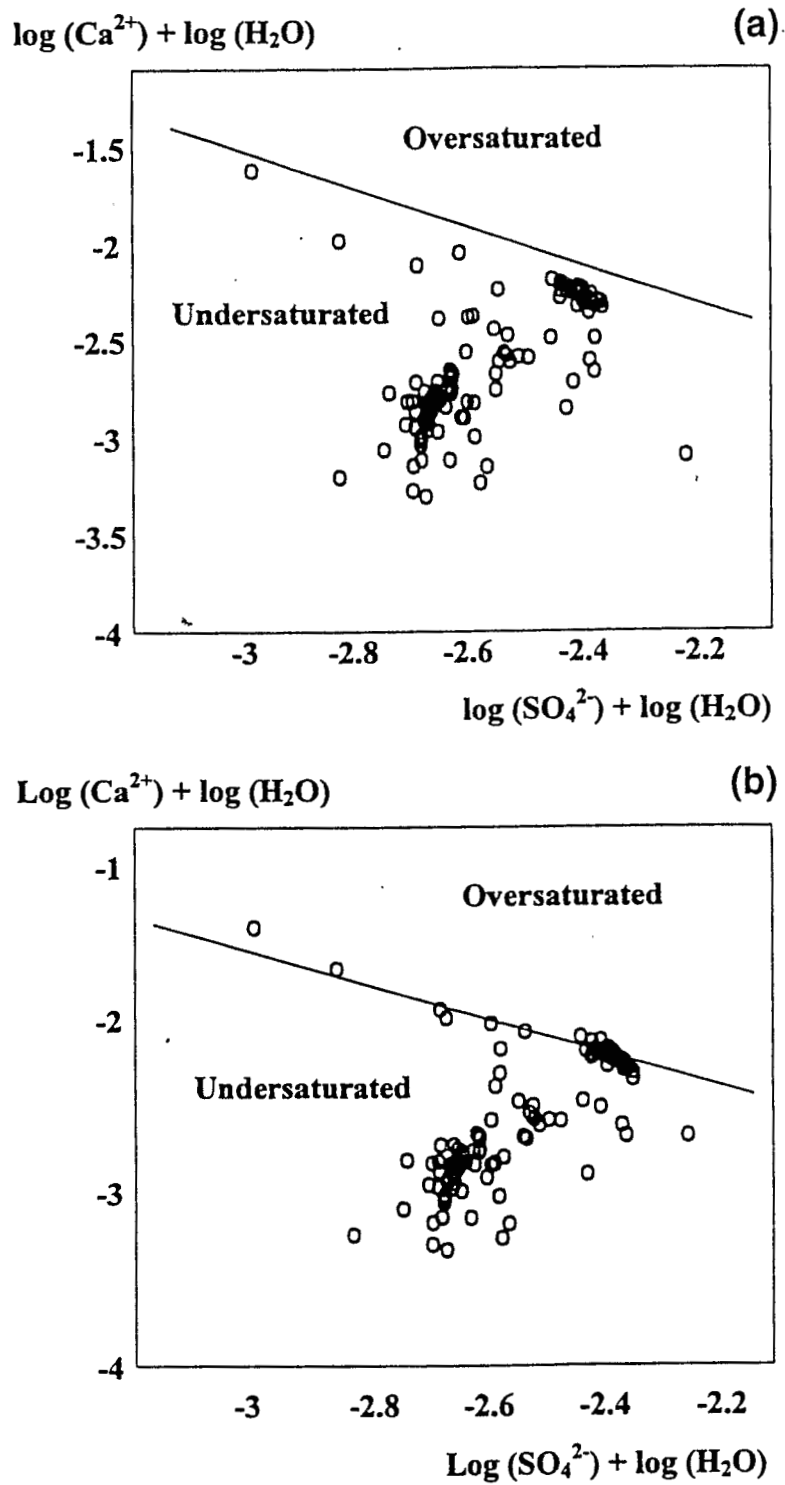
A. Ould Mohamedou et al.

log (Ca^{2+}) + log (H_2O)   **(a)**

Log (Ca^{2+}) + log (H_2O)   **(b)**

FIGURE 6 Saturation diagram with respect to gypsum: (*a*) calculation with the Scatchard extension and (*b*) calculation with the "Aqua" model.
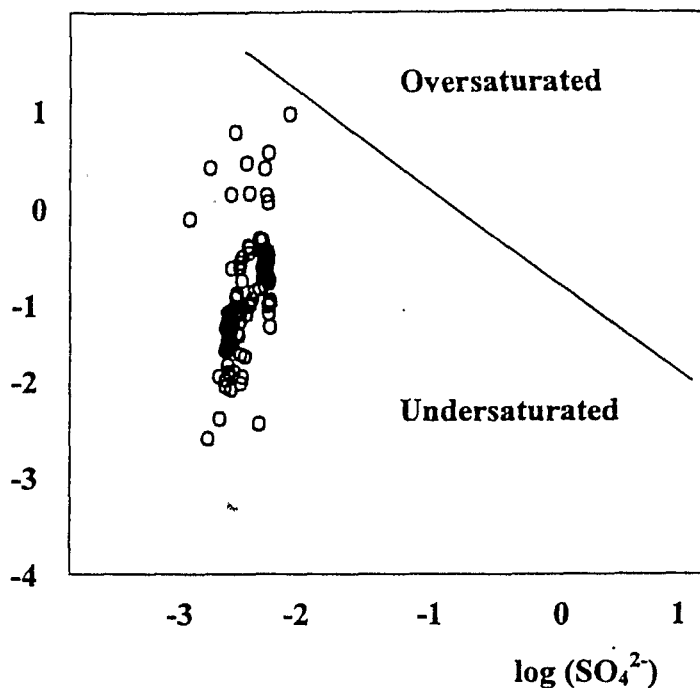
2 log (Na⁺)

FIGURE 7 Saturation diagram with respect to thenardite.

gypsum (Figure 6), thenardite (Figure 7), mirabilite (Figure 8), and halite (Figure 9). Equilibrium was reached with respect to calcite (Figure 5). Some samples exhibit high equilibrating pCO_2, calculated from pH data and alkalinity. It can be attributed to the reaction of calcite with the potential acidity exhibited during oxidation of the soil.

Moderately or very concentrated waters are at saturation with respect to gypsum, while diluted waters are undersaturated with respect to this mineral. The activity calculation according to the Scatchard (1936) extension for the Debye–Hückel law does not make obvious this equilibrium solution/gypsum (Figure 6a). To compensate when the solvent–solute interactions under strong ionic strengths are taken into account, using the "Aqua" model, the points representing moderate and very concentrated solutions are in theoretical equilibrium (Figure 6b). Groundwater and soil extracts are undersaturated with respect to thenardite, mirabilite, or halite (Figures 7, 8, and 9). However, owing to control of sulfate by gypsum precipitation, the equilibrium with respect to halite will probably be reached before the equilibrium with respect to sodium sulfate. It was in agreement with field and SEM observations that only revealed the presence of gypsum and halite.

Residual Alkalinty Used as a Tracer

According to Ribolzi et al. (1996), the residual alkalinity (RA), derived from the identification of the different salts involved during the concentration, behaves theoretically as a tracer. In order to verify that all the precipitation responsible for the

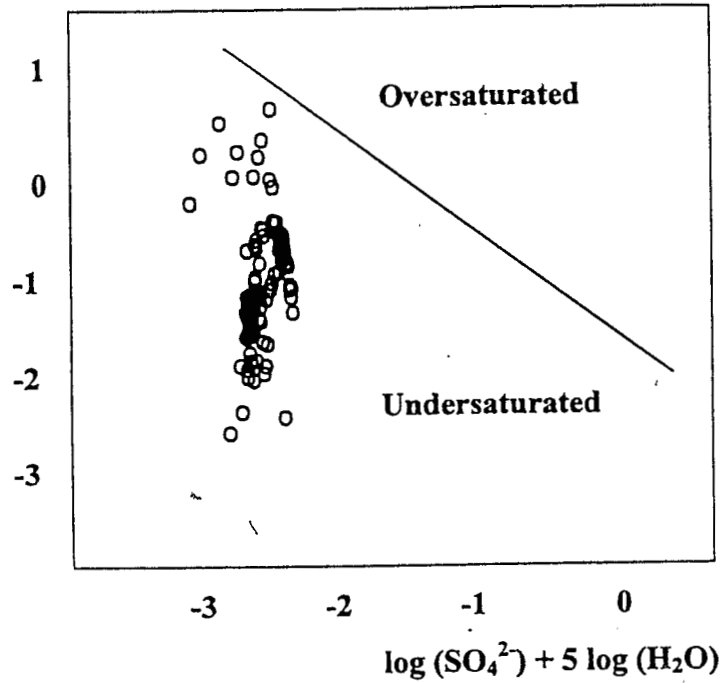*A. Ould Mohamedou et al.*

$$2 \log (Na^+) + 5 \log (H_2O)$$

FIGURE 8 Saturation diagram with respect to mirabilite.
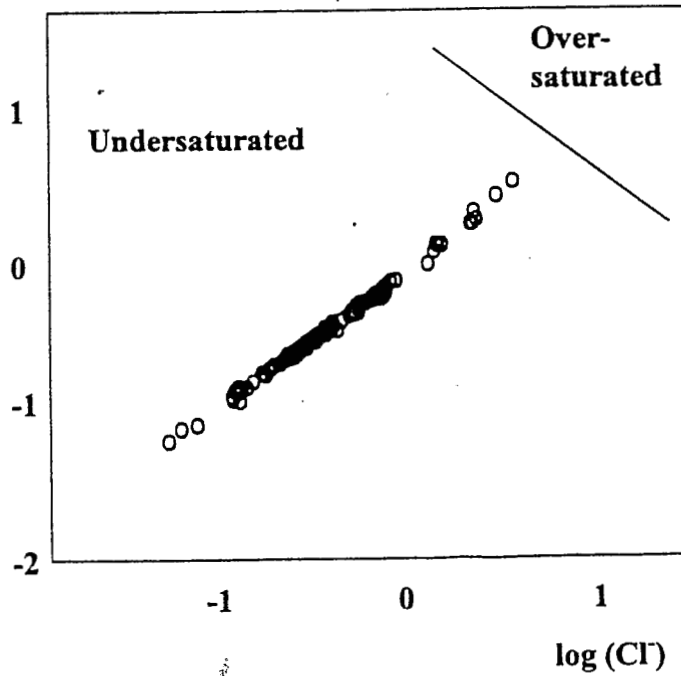
$$\log (Na^+)$$

FIGURE 9 Saturation diagram with respect to halite.

changes in the chemistry of this environment is identified, RA can be compared to amounts of chloride. A close linear relationship ($RA = 1(Cl^-) + B$) is expected. Figure 10 shows the correlation between chloride amounts and RA with respect to gypsum formation,

$$RA_{gypsum} = (SO_4^{2-}) - (Ca^{2+})$$

calcite + gypsum formation,

$$RA_{calcite+gypsum} = Alk. - (Ca^{2+}) + (SO_4^{2-})$$

and calcite + gypsum formation + Na/Ca exchange onto the soil complex:

$$RA_{calcite+gypsum+Na/Ca\ exc.} = Alk. - (Ca^{2+}) + (SO_4^{2-}) + (Na^+)$$

In the first case (Figure 10, correlation *a*), the relationship was fairly close (Table 3), showing that gypsum formation was the main phenomenon responsible for the chemical variability along the concentration process. Nevertheless, some points departed from the straight correlation line. When calcite was considered (Figure 10,
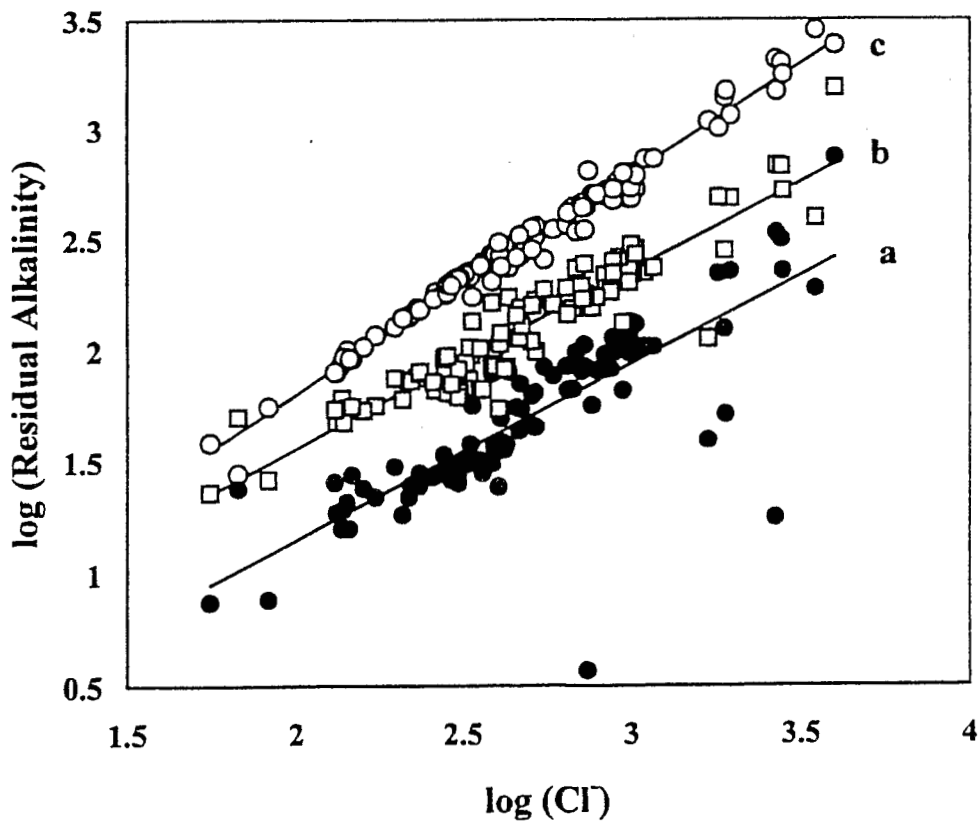

FIGURE 10 Relationships between residual alkalinity and chloride amounts taking into consideration, gypsum (correlation *a*), calcite + gypsum (correlation *b*), and calcite + gypsum + Na/Ca (correlation *c*) exchanges.

TABLE 3 Relationships between residual alkalinity (RA) and chloride amounts

Residual alkalinity, considered components	Relationship	Correlation
Gypsum	RA = 0.79(Cl) − 0.46	$r^2 = 0.65$
Calcite + gypsum	RA = 0.80(Cl) − 0.04	$r^2 = 0.86$
Calcite + gypsum + Na^+/Ca^{2+} exchanges	RA = 0.996(Cl) − 0.18	$r^2 = 0.99$

correlation *b*), the relationship was closer, indicating that the calcite precipitation/ dissolution was involved in the chemical processes, even if the proportions were very low, in agreement with field observations. However, the slope of the scattered plot differs from 1, and this value is only reached when the exchange between Na^+ and Ca^{2+} onto the soil complex is taken into consideration (Figure 10, correlation *c*). In this case, the relationship between RA and Cl^- amounts closely satisfies the theoretical model. We may conclude that the processes responsible for the chemical variability in this environment have been identified.

Conclusion

In the Senegal delta the concentration of ion solutions, under the influence of evaporation, favors a resumption of wind erosion (aeolian deflation and clay dune formation), since the construction of the Diama anti-salting dam.

Although the waters of the Senegal River have a calcic-magnesian carbonated facies, the chemical evolution of the study site corresponds to a neutral evolution, in agreement with the marine origin of the salt. Therefore this type of degradation could not be related to structural effects of the alkaline facies (trona pan) but to production of sand- and silt-sized pelletal aggregates, induced by rapid salt crystallization, especially gypsum and halite (gypsum/halite pan, Bowler, 1973).

All the samples belonged to the same chemical family. The concentration/ dilution of the dissolved elements was identified as the main process responsible for the chemical variability. The minerals precipitated in the order calcite > gypsum > halite. This sequence differed slightly from that described by Valles et al. (1997) in the Aures Chott Meghouane area in Algeria: calcite > gypsum > (celestite) > mirabilite > halite. A similar sequence has been described by Gueddari (1984) in the Chott El Jerid in Tunisia, in which the order was calcite > gypsum > halite > mirabilite, the latter being obtained by artificial concentration. The difference of the studied site is due to the fact that the calcite formation is limited by the acidity arising from the sulfide oxidation of the former mangrove sites.

References

Al Droubi, A., B. Fritz, J. Y. Gac, and Y. Tardy. 1980. Generalized residual alkalinity concept: Application to prediction of the chemical evolution of natural waters by evaporation. *American Journal of Science* 280:560–572.

Boulaine, J. 1954. La sebkha de Ben Ziane et sa lunette ou bourrelet. *Revue de Geomorphologie Dynamique* 5:102–123.

Bourrié, G. 1976. Relations entre le pH, l'alcalinité, le pouvoir tampon et les équilibres de CO_2 dans les eaux naturelles. *Science du Sol* 3:141–159.

Bowler, J. M. 1973. Clay dunes: Their occurrence, formation and environmental signficance. *Earth Science Reviews* 9:315–338.

Eaton, F. M. 1950. Significance of carbonates in irrigation waters. *Soil Science* 69:123–133.

Food and Agriculture Organization. 1994. Draft world reference base for soil resources. FAO, ISRIC, and ISSS, Wageningen and Rome.

Goudie, A. S., and D. S. G. Thomas. 1984. Lunettes in southern Africa. *Journal of Arid Environments* 10:1–12.

Goudie, A. S., and D. S. G. Thomas. 1985. Pans in southern Africa with particular references to South Africa and Zimbabwe. *Zeitschrift für Geomorphologie* 29:1–19.

Gueddari, M. 1984. Géochimie et thermodynamique des évaporites continentales. Etude du lac Natron en Tanzanie et du Chott El Jerid en Tunisie. *Mémoire des Sciences Géologiques* 76:1–143.

Hamdi Aissa, B., N. Fedoroff, and V. Valles. 1997. Short and long term soil system behaviour in hyper arid environment (a case study in the Ouargla Chott, Sahara and Algeria). Presented at the International Symposium on Soil System Behaviour in Time and Space, 19–21 November, Vienna, Austria.

Hills, E. S. 1952. The lunette: A new landform of aeolian origin. *Australian Geographer* 7:1–7.

Lancaster, N. 1978. Composition and formation of southern Kalahari pan margin dunes. *Zeitschrift für Geomorphologie* 22:148–169.

Le Brusq, J. Y., and J. Y. Loyer. 1982. Evolution de la salinité des sols et des eaux en relation avec la riziculture immergée dans le delta du fleuve Sénégal. ORSTOM, Dakar, Senegal.

Le Brusq, J. Y., Loyer, B. Mougenot, and M. Carn. 1987. Nouvelles paragenèses à sulfates d'aluminium, de fer, et de magnésium, et leur distribution dans les sols sulfatés acides du Sénégal. *Science du Sol* 25(3):173–184.

Loyer, J. Y. 1989. Les sols salés de la basse vallée du fleuve Sénégal. Caractérisation, distribution et évolution sous cultures. *Etudes et Thèses*. ORSTOM, Paris.

Marker, M. E., and P. J. Holmes. 1995. Lunettes dunes in the northeast Cape, South Africa, as geomorphic indicators of palaeoenvironmental changes. *Catena* 24:259–273.

Maymard, J. 1952. Les sols du pseudo-delta du Sénégal. Mission d'aménagement du Sénégal. *Bulletin No. 5*. Centre ORSTOM de Dakar-Hann, Dakar, Senegal.

Michel, P. 1973. Les bassins des fleuves Sénégal et Gambie. Etude géomorphologique. *Mémoires ORSTOM 63*. Paris.

Mougenot, B. 1982. Etude pédologique de la cuvette de N'Thiagar, partie Nord, Delta du fleuve Sénégal. ORSTOM, Dakar, Senegal.

Ould Mohamedou, A. 1998. Contribution à l'étude de l'environnement du parc national du Diawling (Mauritanie): Eaux-sols-végétation. Ph.D. thesis, University of Nice–Sophia Antipolis, France.

Pitzer, K. S. 1973. Thermodynamics of electrolytes. I. Theoretical basis and general equation. *Journal of Physical Chemistry* 77:268–277.

Pitzer, K. S. 1975. Thermodynamics of electrolytes. V. Effects of higher order electrostatic terms. *Journal of Soil Chemistry* 4:249–265.

Pitzer, K. S., and J. Kim. 1974. Thermodynamics of electrolytes. IV. Activity and osmotic coefficients for 2-2 electrolytes. *Journal of American Chemical Society* 96:5701–5707.

Price, W. A. 1963. Physicochemical and environmental factors in clay dune genesis. *Journal of Sedimentary Petrology* 33:766–778.

Ribolzi, O., V. Vallès, and L. Barbiéro. 1993. Contrôle géochimique des eaux par la formation de calcite en milieu méditerranéen et en milieu tropical. Arguments d'équilibre et argument de bilan. *Science du Sol* 31:77–95.

Ribolzi, O., V. Vallès, and T. Bariac. 1996. Comparison of hydrograph deconvolutions using residual alkalinity, chloride and oxygen 18 as hydrochemical tracers. *Water Resources Reseach* 32:1051–1059.

Scatchard, G. 1936. Concentrated solutions of strong electrolytes. *Chemistry Review* 19:309–327.

Schecher, W. 1994. MINEQL+: A chemical equilibrium program for personal computers. Environmental Research Software, Hallowell, New Jersey.

Sposito, G. 1988. SOILCHEM: A computer program for the calculation of chemical speciation in soils. Kearney Foundation of Soil Sciences, University of California, Berkeley, California.

Stumm, W., and J. J. Morgan. 1970. *Aquatic chemistry—An introduction emphasising chemical equilibria in natural waters.* Wiley Interscience, New York.

Thomas, D. S. G. 1988. The nature and depositional setting of arid and semiarid Kalahari sediments, southern Africa, *Journal of Arid Environments* 14:17–26.

Thomas, D. S. G., P. A. Nash, P. A. Shaw, and C. Van der Post. 1993. Present day lunette sediment cycling at Witpan in the arid southwestern Kalahari Desert. *Catena* 20:515–527.

Tricart, J. 1954. Influence des sols salés sur la déflation éolienne en basse mauritanie et dans le delta du Sénégal. *Revue de Geomorphologie Dynamique* 5:124–132.

Vallès, V., and F. Bourgeat. 1988. Geochemical determination of the gypsum requirement of cultivated sodic soils. I. Development of the thermodynamic model, "gypsol" simulating the irrigation water-soil chemical interactions. *Arid Soil Research and Rehabilitation* 2:165–177.

Vallès, V., and A. M. De Cockeborne. 1992. Elaboration d'un logiciel de géochimie appliqué à l'étude de la qualité des eaux, pp. 27–30, in *Colloque "Altération et restauration de la qualité des eaux continentales."* Port Leucate.

Vallès, V., Y. A. Pachepsky, and A. A. Ponizovsky. 1991. Invariant criteria for irrigation water quality assessment in arid and semiarid regions, pp. 330–333, in *Genesis and control of fertility of salt affected soils.* ISSS Subcommission on Salt Affected Soils Science, V. V. Dokuchaev Soil Institute, Moscow, Russia.

Vallès, V., M. Rezagui, L. Auque, A. Semadi, L. Roger, and H. Zouggari. 1997. Geochemistry of saline soils in two arid zones of the Mediterranean basin. I. Geochemistry of the Chott Melghir–Mehrouane watershed in Algeria. *Arid Soil Research and Rehabilitation* 11:71–84.

Vallès, V., L. Auque, and P. Lopez. 1999. Proposal to extend Debye–Hückel's law to hyperconcentrated solutions, with application to the brines of the Chott El Jerid (Tunisia) and the salties playas of Aragon (Spain). Submitted for publication to *Chemical Geology.*

van Beek, C. G. E., and N. van Breemen. 1973. The alkalinity of alkali soils. *Journal of Soil Science* 24:129–136.

Vieillefon, J. 1967. Sur l'existence de bourrelets éoliens ou lunettes dans les mangroves de casamance, pp. 436–441, in *Actes congrè panafricain de préhistoire.* Dakar, 6th session. Chambéry, France.

Young, J. A., and R. A. Evans. 1986. Erosion and deposition of fine sediments from playas. *Journal of Arid Environments* 10:103–116.